Journal of Computational and Applied Mathematics 389 (2021) 113330

Contents lists available at ScienceDirect

Journal of Computational and Applied Mathematics

journal homepage: www.elsevier.com/locate/cam

The virtual element method for general elliptic hemivariational inequalities

Fei Wang [a,*,1], Bangmin Wu [a], Weimin Han [b]

[a] School of Mathematics and Statistics, Xi'an Jiaotong University, Xi'an, Shaanxi 710049, China
[b] Department of Mathematics & Program in Applied Mathematical and Computational Sciences, University of Iowa, Iowa City, IA 52242, USA

ARTICLE INFO

Article history:
Received 29 April 2020
Received in revised form 3 November 2020

MSC:
65N30
65N15
74M10
74M15

Keywords:
Elliptic hemivariational inequality
Virtual element method
Error estimates
Contact mechanics

ABSTRACT

An abstract framework of the virtual element method is established for solving general elliptic hemivariational inequalities with or without constraint, and a unified a priori error analysis is given for both cases. Then, virtual element methods of arbitrary order are applied to solve three elliptic hemivariational inequalities arising in contact mechanics, and optimal order error estimates are shown with the linear virtual element solutions. Numerical simulation results are reported in several contact problems; in particular, the numerical convergence orders of the lowest order virtual element solutions are shown to be in good agreement with the theoretical predictions.

1. Introduction

In physical and engineering sciences, many problems are modeled by partial differential equations with proper boundary and/or initial conditions. More complex physical processes have been studied as variational inequalities (VIs), which form an important and very useful class of nonlinear problems arising in diverse application areas of physical, engineering, financial, and management sciences; some early references on modeling, mathematical theory and numerical analysis of variational inequalities include [1–6].

Variational inequalities are mathematical problems with convex structures. For problems involving nonsmooth and non-convex relations, hemivariational inequalities arise. In 1983, Panagiotopoulos [7] coined the notion of hemivariational inequalities, which is closely related to the concept of the generalized gradient of a locally Lipschitz function (allowed to be non-convex) introduced by Clarke [8,9]. Since then, it has been shown that hemivariational inequalities are a powerful tool for many applications in areas such as nonsmooth mechanics, physics, engineering, and economics. For this reason, publications on hemivariational inequalities are growing rapidly, and the mathematical theory and applications of hemivariational inequalities can be found in several books [10–14] and the references therein. In comparison, systematic analysis of numerical methods for solving hemivariational inequalities is more recent. A comprehensive reference on the finite element method for hemivariational inequalities is [15], where convergences of some numerical schemes were shown, but no error estimate was derived. In [16], an optimal order error estimate was derived for the numerical solution

* Corresponding author.
E-mail addresses: feiwang.xjtu@xjtu.edu.cn (F. Wang), wbmlll123456@stu.xjtu.edu.cn (B. Wu), weimin-han@uiowa.edu (W. Han).
1 The work of this author was partially supported by the National Natural Science Foundation of China (Grant No. 11771350).

https://doi.org/10.1016/j.cam.2020.113330
0377-0427/

of a hemivariational inequality with the linear finite element. Since then, there have been various developments on convergences of numerical solutions under basic solution regularity and optimal order error estimates for linear finite element solutions under suitable solution regularity assumptions for hemivariational inequalities; see a recent summary account [17].

In recent years, as an extension of the classical finite element method, the virtual element method (VEM) has been developed [18] and applied for solving a variety of partial differential equations; in particular, it was used to solve linear elasticity problems, e.g., [19–22]. The virtual element space consists of polynomials up to a certain degree and some additional non-polynomial functions, and VEM is flexible in handling very general (non-convex) polygonal elements with an arbitrary number of edges. Furthermore, the h adaptive strategy is very suitable for VEM because it treats the geometrical hanging nodes as the vertices of the polygonal elements. In the VEM framework, the stiffness matrix is calculated without actually computing the non-polynomial functions with the help of proper projection operators. In [23], the virtual element method was applied to solve a contact problem; however, there was no error estimate. In [24,25], the VEMs were studied for solving an obstacle problem and a simplified friction problem, respectively, and error estimates were established. This appears to be the first time in the literature where the optimal first-order error estimate is established for the lowest-order virtual element method for solving variational inequalities. In [26], the virtual element method was studied for solving elliptic variational inequalities of the second kind. In [27], a general framework was established to study the conforming and nonconforming virtual element methods for solving a Kirchhoff plate contact problem with friction, which is a fourth-order elliptic variational inequality of the second kind. In a unified framework, a priori error estimates were derived for these virtual elements, and they achieve the optimal convergence order for the lowest-order case. In [28], the lowest order VEM was developed and analyzed for solving an elliptic hemivariational inequality without constraint. In this paper, we establish an abstract framework of VEM for solving general elliptic hemivariational inequalities with or without constraint and provide a unified a priori error analysis for both cases (with and without constraint). Then, we apply the VEM of arbitrary order to three HVIs arising from contact mechanics and show that the lowest order VEM achieves the optimal convergence order. In general, optimal error estimates cannot be derived for high-order methods due to the presence of error bound terms on the contact boundary. However, with proper solution regularity assumptions, if we refine the elements along the contact boundary, the optimal convergence order will be possible through adding certain degrees of freedom (cf. Remark 5.1), and such meshes can be easily created with the virtual element framework. It is one advantage of using VEM to solve contact problems.

The rest of the paper is organized as follows: In Section 2, we introduce some notation and a general family of elliptic hemivariational inequalities with and without constraints. In Section 3, we introduce the framework of the virtual element method for solving the hemivariational inequalities and derive Céa-type inequalities for error estimation. Then in the remaining sections, we discuss the application of the virtual element method to solve the three contact problems in two-dimensions. In Section 4, we describe the construction of the virtual element. In Section 5, we apply the earlier error analysis to three contact problems, in which the material's behavior is modeled with a linearly elastic constitutive law and contact conditions in subdifferential forms. Optimal first-order error estimates are shown for the lowest-order virtual element method under suitable solution regularity assumptions. Finally, in Section 6, we present some numerical results which support the theoretical error estimates.

2. Elliptic hemivariational inequality

2.1. Preliminaries

Given a bounded domain $D \subset \mathbb{R}^d$, let V be a function space defined on D with the norm $\|\cdot\|_{V,D}$, which is usually written as $\|\cdot\|_V$. Denote its topological dual by V^*, and the collection of all the subsets of V^* by 2^{V^*}. The duality pairing between V and V^* is denoted by $\langle\cdot,\cdot\rangle_{V^*\times V}$, or simply $\langle\cdot,\cdot\rangle$ where no confusion may arise. Given two normed spaces, V and W, let $\mathcal{L}(V,W)$ be the space of all continuous linear operators from V to W.

We recall the definitions of the convex and the Clarke subdifferentials.

Definition 2.1. Let $\varphi\colon V\to\mathbb{R}\cup\{+\infty\}$ be a proper, convex and lower semicontinuous function. The mapping $\partial_c\varphi\colon V\to 2^{V^*}$ defined by

$$\partial_c\varphi(u):=\{u^*\in V^*:\langle u^*,v-u\rangle\le\varphi(v)-\varphi(u)\quad\forall\,v\in V\}$$

is called the (convex) subdifferential of φ. If $\partial_c\varphi(u)$ is non-empty, any element $u^*\in\partial_c\varphi(u)$ is called a subgradient of φ at u.

Definition 2.2. Let $\psi\colon V\to\mathbb{R}$ be a locally Lipschitz function. The generalized (Clarke) directional derivative of ψ at $u\in V$ in the direction $v\in V$ is defined by

$$\psi^0(u;v):=\limsup_{w\to u,\ \lambda\downarrow 0}\frac{\psi(w+\lambda v)-\psi(w)}{\lambda}.$$

The generalized gradient (subdifferential) of ψ at u is defined by

$$\partial\psi(u):=\left\{\zeta\in V^*:\psi^0(u;v)\ge\langle\zeta,v\rangle\quad\forall\,v\in V\right\}.$$

Details on the properties of the subdifferential mappings, both in the convex and Clarke sense, can be found in the books [9,11,13,29]. In particular, knowing the generalized subdifferential, we can compute the generalized directional derivative through the formula [9]

$$\psi^0(u; v) = \max\{\langle \zeta, v\rangle : \zeta \in \partial\psi(u)\}. \tag{2.1}$$

The generalized directional derivative is subadditive with respect to the direction variable:

$$\psi^0(u; v_1 + v_2) \le \psi^0(u; v_1) + \psi^0(u; v_2) \quad \forall\, u, v_1, v_2 \in V. \tag{2.2}$$

2.2. A general elliptic hemivariational inequality

Let V be a reflexive Banach space, K a closed and convex subset of V with $0_V \in K$, and V_j a Banach space. Given a symmetric bilinear form $a(\cdot,\cdot) : V \times V \to \mathbb{R}$, a functional $j: V_j \to \mathbb{R}$, a linear operator $\gamma_j : V \to V_j$ and $f \in V^*$, a general elliptic hemivariational inequality is as follows:

Problem 2.3. Find an element $u \in K$ such that

$$a(u, v - u) + j^0(\gamma_j u; \gamma_j v - \gamma_j u) \ge \langle f, v - u\rangle \quad \forall\, v \in K. \tag{2.3}$$

As a particular case, when $K = V$, (2.3) is an elliptic hemivariational inequality without constraint.

To study Problem 2.3, we make the following assumptions:

Assumption 2.4. (A_1) The linear operator $\gamma_j \in \mathcal{L}(V, V_j)$, and we denote by $c_j > 0$ an upper bound of $\|\gamma_j\|$:

$$\|\gamma_j v\|_{V_j} \le c_j \|v\|_V \quad \forall\, v \in V. \tag{2.4}$$

(A_2) There are constants $m > 0$ and $M > 0$ such that

$$a(v, v) \ge m\|v\|_V^2 \quad \forall\, v \in V, \tag{2.5}$$

$$a(u, v) \le M\|u\|_V\|v\|_V \quad \forall\, u, v \in V. \tag{2.6}$$

(A_3) $j: V_j \to \mathbb{R}$ is locally Lipschitz, and there are constants $c_0, c_1, \alpha_j \ge 0$ such that

$$\|\partial j(z)\|_{V_j^*} \le c_0 + c_1\|z\|_{V_j} \quad \forall\, z \in V_j, \tag{2.7}$$

$$j^0(z_1; z_2 - z_1) + j^0(z_2; z_1 - z_2) \le \alpha_j\|z_1 - z_2\|_{V_j}^2 \quad \forall\, z_1, z_2 \in V_j. \tag{2.8}$$

(A_4) The smallness condition holds

$$\alpha_j c_j^2 < m. \tag{2.9}$$

Remark 2.5. If we define an operator $A: V \to V^*$ related to the bilinear form $a(u, v)$ by

$$a(u, v) = \langle Au, v\rangle,$$

then (2.5)–(2.6) implies that A is Lipschitz continuous, pseudomonotone and strongly monotone, i.e.,

$$\|Au - Av\|_{V^*} \le M\|u - v\|_V \quad \forall\, u, v \in V,$$

$$\langle Av_1 - Av_2, v_1 - v_2\rangle \ge m\|v_1 - v_2\|_V^2 \quad \forall\, v_1, v_2 \in V.$$

Remark 2.6. For contact problems leading to the hemivariational inequalities, the functional $j(\cdot)$ is an integral over the contact boundary Γ_3, and V_j can be chosen to be $L^2(\Gamma_3)$ or $L^2(\Gamma_3)^d$. The smallness assumption (2.9) poses a limit on the degree of the non-convexity of j relative to the strong monotonicity of the bilinear form. When $j: V_j \to \mathbb{R}$ is convex, (2.8) holds with $\alpha_j = 0$ due to the monotonicity of the convex subdifferential.

In [30], the following existence and uniqueness result was proved.

Theorem 2.7. *Under Assumption 2.4, Problem 2.3 has a unique solution $u \in K$.*

Moreover, the assumption $0_V \in K$ can be replaced by non-emptiness of K [30].

2.3. Contact problems

Consider the contact between a linearly elastic body and a foundation. Let the initial configuration of the linearly elastic body be an open, bounded, Lipschitz domain $\Omega \subset \mathbb{R}^d$ $(d = 2, 3)$. The boundary $\Gamma = \partial\Omega$ is partitioned into three disjoint and measurable parts Γ_1, Γ_2 and Γ_3 such that $\mathrm{meas}(\Gamma_1) > 0$. Denote the displacement field by $\boldsymbol{u}: \Omega \to \mathbb{R}^d$ and the stress field by $\boldsymbol{\sigma}\colon \Omega \to \mathbb{S}^d$, the space of second order symmetric tensors on $\mathbb{R}^d$ with the inner product $\boldsymbol{\sigma} : \boldsymbol{\tau} = \sigma_{ij}\,\tau_{ij}$. The linearized strain tensor associated with $\boldsymbol{u}$ is defined by

$$\boldsymbol{\varepsilon}(\boldsymbol{u}) = \frac{1}{2}\left(\nabla\boldsymbol{u} + (\nabla\boldsymbol{u})^T\right).$$

The unit outward normal vector $\boldsymbol{\nu}$ on Γ exists a.e. since Ω is a Lipschitz domain. For a vector-valued function $\boldsymbol{v}$, we use $v_\nu := \boldsymbol{v}\cdot\boldsymbol{\nu}$ and $\boldsymbol{v}_\tau := \boldsymbol{v} - v_\nu\boldsymbol{\nu}$ for the normal and tangential components of $\boldsymbol{v}$ on the boundary. Similarly, for the stress field $\boldsymbol{\sigma}$, its normal and tangential components on Γ are defined as $\sigma_\nu := (\boldsymbol{\sigma}\boldsymbol{\nu})\cdot\boldsymbol{\nu}$ and $\boldsymbol{\sigma}_\tau := \boldsymbol{\sigma}\boldsymbol{\nu} - \sigma_\nu\boldsymbol{\nu}$, respectively.

Given $\boldsymbol{f}_1 \in L^2(\Omega;\mathbb{R}^d)$ and $\boldsymbol{f}_2 \in L^2(\Gamma_2;\mathbb{R}^d)$, the contact problem is to find a displacement field $\boldsymbol{u}\colon \Omega \to \mathbb{R}^d$ and a stress field $\boldsymbol{\sigma}\colon \Omega \to \mathbb{S}^d$ such that

$$\boldsymbol{\sigma}(\boldsymbol{u}) = \mathcal{C}\boldsymbol{\varepsilon}(\boldsymbol{u}) \quad \text{in } \Omega, \tag{2.10}$$

$$-\nabla\cdot\boldsymbol{\sigma}(\boldsymbol{u}) = \boldsymbol{f}_1 \quad \text{in } \Omega, \tag{2.11}$$

$$\boldsymbol{u} = \boldsymbol{0} \quad \text{on } \Gamma_1, \tag{2.12}$$

$$\boldsymbol{\sigma}\boldsymbol{\nu} = \boldsymbol{f}_2 \quad \text{on } \Gamma_2, \tag{2.13}$$

together with a set of contact boundary conditions on Γ_3. Different contact conditions will lead to different contact problems. Here, (2.10) is the linearly elastic constitutive law. As usual, the elasticity operator $\mathcal{C} = (\mathcal{C}_{ijkl})\colon \mathbb{S}^d \to \mathbb{S}^d$ is assumed to be bounded, symmetric, and pointwise stable:

$$\begin{cases} \text{(a) } L_{\mathcal{C}} = \|\mathcal{C}\| < \infty; \\ \text{(b) } \mathcal{C}_{ijkl} = \mathcal{C}_{jikl} = \mathcal{C}_{klij}, \quad 1 \le i,j,k,l \le d; \\ \text{(c) } \mathcal{C}_{ijkl}\varepsilon_{ij}\varepsilon_{kl} \ge m_{\mathcal{C}}\|\boldsymbol{\varepsilon}\|^2. \end{cases} \tag{2.14}$$

The relations (2.11)–(2.13) mean that the elastic body is fixed on Γ_1, and is in equilibrium under the action of volume forces of a total density $\boldsymbol{f}_1$ in Ω and surface tractions of a total density $\boldsymbol{f}_2$ on Γ_2. Furthermore, the elastic body is in potential contact on Γ_3 with a foundation. Here and below we do not always display explicitly the dependence of a quantity on the spatial variable $\boldsymbol{x}$.

To study the contact problems, we introduce the function space

$$W = \left\{\boldsymbol{v} \in H^1(\Omega;\mathbb{R}^d) : \boldsymbol{v} = \boldsymbol{0} \text{ a.e. on } \Gamma_1\right\}. \tag{2.15}$$

Since $\mathrm{meas}\,(\Gamma_1) > 0$, it is known that W is a Hilbert space with the inner product

$$(\boldsymbol{u},\boldsymbol{v})_W := \int_\Omega \boldsymbol{\varepsilon}(\boldsymbol{u}) : \boldsymbol{\varepsilon}(\boldsymbol{v})\,dx \quad \forall\,\boldsymbol{u},\boldsymbol{v} \in W$$

and the associated norm $\|\cdot\|_W$. For $\boldsymbol{v} \in H^1(\Omega;\mathbb{R}^d)$, the same symbol $\boldsymbol{v}$ is used for its trace on Γ, and we have a constant $c > 0$ such that

$$\|\boldsymbol{v}\|_{L^2(\Gamma_3;\mathbb{R}^d)} \le c\,\|\boldsymbol{v}\|_W \quad \forall\,\boldsymbol{v} \in W,$$

by the trace theorem. In addition, we define $\boldsymbol{f} \in W^*$ by

$$\langle \boldsymbol{f},\boldsymbol{v}\rangle_{W^*\times W} = (\boldsymbol{f}_1,\boldsymbol{v})_{L^2(\Omega;\mathbb{R}^d)} + (\boldsymbol{f}_2,\boldsymbol{v})_{L^2(\Gamma_2;\mathbb{R}^d)} \quad \forall\,\boldsymbol{v} \in W. \tag{2.16}$$

As examples of Problem 2.3, with the relations (2.10)–(2.13), we consider three choices of the contact boundary conditions on Γ_3, leading to three hemivariational inequalities below.

2.3.1. A bilateral contact problem with friction

Given a potential function $j_\tau\colon \Gamma_3 \times \mathbb{R}^d \to \mathbb{R}$, the first set of contact boundary conditions we consider is

$$u_\nu = 0, \quad -\boldsymbol{\sigma}_\tau \in \partial j_\tau(\boldsymbol{u}_\tau) \quad \text{on } \Gamma_3. \tag{2.17}$$

The first relation in (2.17) is the bilateral contact condition, and the second relation indicates that the contact is frictional. In Problem (2.3), let

$$K = V := \{\boldsymbol{v} \in W : v_\nu = 0 \text{ a.e. on } \Gamma_3\}, \tag{2.18}$$

$$V_j = L^2(\Gamma_3;\mathbb{R}^d), \quad \gamma_j\boldsymbol{v} = \boldsymbol{v}_\tau \text{ for } \boldsymbol{v} \in V, \tag{2.19}$$

and define a bilinear form

$$a(\boldsymbol{u},\boldsymbol{v}) = \int_\Omega \boldsymbol{\sigma}(\boldsymbol{u}) : \boldsymbol{\varepsilon}(\boldsymbol{v})\,dx \quad \forall\,\boldsymbol{u},\boldsymbol{v} \in V \tag{2.20}$$

as well as a functional

$$j(\boldsymbol{z}) = \int_{\Gamma_3} j_\tau(\cdot,\boldsymbol{z}(\cdot))\,ds \quad \forall\,\boldsymbol{z} \in L^2(\Gamma_3;\mathbb{R}^d). \tag{2.21}$$

Assume the potential function $j_\tau\colon \Gamma_3 \times \mathbb{R}^d \to \mathbb{R}$ has the following properties:

$$\begin{cases} \text{(a) } j_\tau(\cdot, \boldsymbol{z}) \text{ is measurable on } \Gamma_3 \text{ for all } \boldsymbol{z} \in \mathbb{R}^d \text{ and } j_\tau(\cdot, \boldsymbol{0}) \in L^1(\Gamma_3); \\ \text{(b) } j_\tau(\boldsymbol{x}, \cdot) \text{ is locally Lipschitz on } \mathbb{R}^d \text{ for a.e. } \boldsymbol{x} \in \Gamma_3; \\ \text{(c) } |\partial j_\tau(\boldsymbol{x}, \boldsymbol{z})| \le c_{\tau,0} + c_{\tau,1}\|\boldsymbol{z}\| \text{ for a.e. } \boldsymbol{x} \in \Gamma_3, \\ \qquad \text{for all } \boldsymbol{z} \in \mathbb{R}^d \text{ with } c_{\tau,0},\ c_{\tau,1} \ge 0; \\ \text{(d) } j_\tau^0(\boldsymbol{x}, \boldsymbol{z}_1; \boldsymbol{z}_2 - \boldsymbol{z}_1) + j_\tau^0(\boldsymbol{x}, \boldsymbol{z}_2; \boldsymbol{z}_1 - \boldsymbol{z}_2) \le \alpha_{j_\tau} \|\boldsymbol{z}_1 - \boldsymbol{z}_2\|^2 \\ \qquad \text{for a.e. } \boldsymbol{x} \in \Gamma_3,\ \text{all } \boldsymbol{z}_1, \boldsymbol{z}_2 \in \mathbb{R}^d \text{ with } \alpha_{j_\tau} \ge 0. \end{cases} \tag{2.22}$$

Then it can be shown that the functional j defined by (2.21) satisfies the assumption (A_3) with $\alpha_j = \alpha_{j_\tau}$.

The weak formulation of the contact problem is as follows:

Problem (P_1). Find a displacement field $\boldsymbol{u} \in V$ such that

$$a(\boldsymbol{u}, \boldsymbol{v}) + \int_{\Gamma_3} j_\tau^0(\boldsymbol{u}_\tau; \boldsymbol{v}_\tau)\, ds \ge \langle \boldsymbol{f}, \boldsymbol{v}\rangle_{V^* \times V} \quad \forall\, \boldsymbol{v} \in V. \tag{2.23}$$

Assume the smallness condition (2.9) that takes the form $\alpha_{j_\tau} < \lambda_{1,V}^{1/2} m_{\mathcal{C}}$ for the contact problem under consideration, where $\lambda_{1,V} > 0$ is the smallest eigenvalue of the eigenvalue problem

$$\boldsymbol{u} \in W, \quad \int_\Omega \boldsymbol{\varepsilon}(\boldsymbol{u}) : \boldsymbol{\varepsilon}(\boldsymbol{v})\, dx = \lambda \int_{\Gamma_3} \boldsymbol{u}_\tau \cdot \boldsymbol{v}_\tau\, ds \quad \forall\, \boldsymbol{v} \in W.$$

Then applying Theorem 2.7, we know that Problem (P_1) has a unique solution [30].

2.3.2. A frictionless normal compliance contact problem

Given a potential function $j_\nu\colon \Gamma_3 \times \mathbb{R} \to \mathbb{R}$, the second set of contact boundary conditions is

$$-\sigma_\nu \in \partial j_\nu(u_\nu), \quad \boldsymbol{\sigma}_\tau = \boldsymbol{0} \quad \text{on } \Gamma_3. \tag{2.24}$$

The first relation in (2.24) is a normal compliance contact condition, whereas the frictionless contact feature is reflected by the condition $\boldsymbol{\sigma}_\tau = \boldsymbol{0}$. Then the weak formulation of the second contact problem is the following:

Problem (P_2). Find a displacement field $\boldsymbol{u} \in V$ such that

$$a(\boldsymbol{u}, \boldsymbol{v}) + \int_{\Gamma_3} j_\nu^0(u_\nu; v_\nu)\, ds \ge \langle \boldsymbol{f}, \boldsymbol{v}\rangle_{V^* \times V} \quad \forall\, \boldsymbol{v} \in V. \tag{2.25}$$

This problem is a special case of Problem 2.3 with the following setting:

$$K = V = W, \quad V_j = L^2(\Gamma_3), \quad \gamma_j \boldsymbol{v} = v_\nu \text{ for } \boldsymbol{v} \in V, \tag{2.26}$$

$$j(z) = \int_{\Gamma_3} j_\nu(\cdot, z(\cdot))\, ds, \quad z \in L^2(\Gamma_3). \tag{2.27}$$

Assume the potential function $j_\nu\colon \Gamma_3 \times \mathbb{R} \to \mathbb{R}$ has the following properties:

$$\begin{cases} \text{(a) } j_\nu(\cdot, z) \text{ is measurable on } \Gamma_3 \text{ for all } z \in \mathbb{R} \text{ and } j_\nu(\cdot, 0) \in L^1(\Gamma_3); \\ \text{(b) } j_\nu(\boldsymbol{x}, \cdot) \text{ is locally Lipschitz on } \mathbb{R} \text{ for a.e. } \boldsymbol{x} \in \Gamma_3; \\ \text{(c) } |\partial j_\nu(\boldsymbol{x}, z)| \le c_{\nu,0} + c_{\nu,1}|z| \text{ for a.e. } \boldsymbol{x} \in \Gamma_3, \\ \qquad \text{for all } z \in \mathbb{R} \text{ with } c_{\nu,0},\ c_{\nu,1} \ge 0; \\ \text{(d) } j_\nu^0(\boldsymbol{x}, z_1; z_2 - z_1) + j_\nu^0(\boldsymbol{x}, z_2; z_1 - z_2) \le \alpha_{j_\nu} |z_1 - z_2|^2 \\ \qquad \text{for a.e. } \boldsymbol{x} \in \Gamma_3,\ \text{all } z_1, z_2 \in \mathbb{R} \text{ with } \alpha_{j_\nu} \ge 0. \end{cases} \tag{2.28}$$

Then $j(z)$ defined by (2.27) satisfies (A_3). The smallness assumption (2.9) now takes the form $\alpha_{j_\nu} < \lambda_{2,V}^{1/2} m_{\mathcal{C}}$, where $\lambda_{2,V} > 0$ is the smallest eigenvalue of the eigenvalue problem

$$\boldsymbol{u} \in W, \quad \int_\Omega \boldsymbol{\varepsilon}(\boldsymbol{u}) : \boldsymbol{\varepsilon}(\boldsymbol{v})\, dx = \lambda \int_{\Gamma_3} u_\nu v_\nu\, ds \quad \forall\, \boldsymbol{v} \in W.$$

Then it can be shown that Problem (P_2) has a unique solution $\boldsymbol{u} \in V$ by Theorem 2.7 [30].

2.3.3. A frictionless unilateral contact problem

The third set of contact boundary conditions is

$$u_\nu \le g,\ \sigma_\nu + \xi_\nu \le 0,\ (u_\nu - g)(\sigma_\nu + \xi_\nu) = 0,\ \xi_\nu \in \partial j_\nu(u_\nu) \quad \text{on } \Gamma_3, \tag{2.29}$$

$$\boldsymbol{\sigma}_\tau = \boldsymbol{0} \quad \text{on } \Gamma_3, \tag{2.30}$$

which models frictionless contact of the elastic body with a foundation made of a rigid body covered by a layer made of elastic material. Penetration is restricted by the relation $u_\nu \leq g$, where g represents the thickness of the elastic layer. When there is penetration and the normal displacement does not reach the bound g, the contact is described by a multivalued normal compliance condition: $-\sigma_\nu = \xi_\nu \in \partial j_\nu(u_\nu)$.

Corresponding to the constraint $u_\nu \leq g$ on Γ_3, we introduce a subset of the space W of (2.15):

$$U := \{\boldsymbol{v} \in W : v_\nu \leq g \text{ on } \Gamma_3\}. \tag{2.31}$$

The weak formulation of the contact problem is the following.

Problem (P$_3$). Find a displacement field $\boldsymbol{u} \in U$ such that

$$a(\boldsymbol{u}, \boldsymbol{v} - \boldsymbol{u}) + \int_{\Gamma_3} j_\nu^0(u_\nu; v_\nu - u_\nu)\, ds \geq \langle \boldsymbol{f}, \boldsymbol{v} - \boldsymbol{u} \rangle_{V^* \times V} \quad \forall \boldsymbol{v} \in U. \tag{2.32}$$

To apply Theorem 2.7, we let

$$V = W, \quad K = U, \quad V_j = L^2(\Gamma_3), \quad \gamma_j \boldsymbol{v} = v_\nu \text{ for } \boldsymbol{v} \in V,$$

Assuming the smallness condition $\alpha_{j_\nu} < \lambda_{2,V}^{1/2} m_{\mathcal{C}}$, it can be shown that Problem (P$_3$) has a unique solution $\boldsymbol{u} \in U$ under proper assumptions [30].

3. Virtual element method

In this section, we follow the ideas in [18,19] to set up the abstract framework of the virtual element method for solving Problem 2.3. We keep Assumption 2.4 so that Problem 2.3 has a unique solution $u \in K$.

3.1. Abstract framework

Given a bounded polygonal domain Ω and let $\mathcal{T}^h$ be a decomposition of $\overline{\Omega}$ into elements denoted by T. Let $h_T = \mathrm{diam}(T)$ and $h = \max\{h_T : T \in \mathcal{T}^h\}$. We assume that the bilinear form $a(u, v)$ is defined on the domain Ω, and can be split as

$$a(u, v) = \sum_{T \in \mathcal{T}^h} a_T(u, v),$$

where $a_T(u, v)$ is the restriction of $a(u, v)$ on T, and

$$a_T(u, v) \leq M \|u\|_{V,T} \|v\|_{V,T} \quad \forall\, u, v \in V_T. \tag{3.1}$$

Here, V_T is the restriction of V on T. In addition, we assume that the virtual element space $V^h \subset V$ and the bilinear form a^h satisfy the following assumptions:

Assumption 3.1. For each h, there exists an element $f^h \in (V^h)^*$ such that

$$\|f^h\|_{(V^h)^*} = \sup_{v^h \in V^h} \frac{\langle f^h, v^h \rangle}{\|v^h\|_V}$$

is uniformly bounded, and a symmetric bilinear form $a^h(\cdot,\cdot) : V^h \times V^h \to \mathbb{R}$ such that

$$a^h(u^h, v^h) = \sum_{T \in \mathcal{T}^h} a_T^h(u^h, v^h), \tag{3.2}$$

where $a_T^h(\cdot,\cdot)$ is a bilinear form on $V_T^h \times V_T^h$ with V_T^h is the restriction of V^h on T. Furthermore, for each T, we have $\mathbb{P}_k(T) \subset V_T^h$, and the bilinear form a_T^h has the following properties:

(i) k-**consistency:**

$$a_T^h(v^h, p) = a_T(v^h, p) \quad \forall\, v^h \in V_T^h,\ p \in \mathbb{P}_k(T); \tag{3.3}$$

(ii) **stability:** there exist two positive constants α_* and α^*, independent of h and T, s.t.

$$\alpha_* a_T(v^h, v^h) \leq a_T^h(v^h, v^h) \leq \alpha^* a_T(v^h, v^h) \quad \forall\, v^h \in V_T^h. \tag{3.4}$$

The symmetry of $a^h(\cdot,\cdot)$, stability (3.4) and the continuity (3.1) of $a_T(\cdot,\cdot)$ easily imply the continuity

$$a_T^h(u^h, v^h) \leq \alpha^* M \|u^h\|_{V,T} \|v^h\|_{V,T} \quad \forall\, u^h, v^h \in V_T^h. \tag{3.5}$$

In addition, from (3.2), (3.4) and (3.5), it follows that

$$\alpha_* a(v^h, v^h) \leq a^h(v^h, v^h) \leq \alpha^* a(v^h, v^h) \quad \forall\, v^h \in V^h, \tag{3.6}$$

$$a^h(u^h, v^h) \le \alpha^* M \|u^h\|_{V,h} \|v^h\|_{V,h} \quad \forall\, u^h, v^h \in V^h. \tag{3.7}$$

Here, $\|\cdot\|_{V,h} = \left(\sum_{T\in\mathcal{T}^h} \|\cdot\|_{V,T}^2\right)^{1/2}$.

In the rest of the paper, we will use $c > 0$ to represent a generic constant that is independent of the mesh size h, and it may take different values at different appearances.

3.2. Virtual element scheme for HVI with constraint

We use $K^h := V^h \cap K$ to approximate the convex set K. The virtual element method for solving Problem 2.3 is the following.

Problem 3.2. *Find $u^h \in K^h$ such that*

$$a^h(u^h, v^h - u^h) + j^0(\gamma_j u^h; \gamma_j v^h - \gamma_j u^h) \ge \langle f^h, v^h - u^h\rangle \quad \forall\, v^h \in K^h. \tag{3.8}$$

Remark 3.3. With Assumption 2.4 and a further assumption $\alpha_* m > \alpha_j c_j^2$ replacing (2.9), we can prove that Problem 3.2 has a unique solution $u^h \in K^h$. Indeed, defining $A^h\colon V^h \to (V^h)^*$ by the relation

$$\langle A^h u, v\rangle := a^h(u, v) \quad \forall\, u, v \in V^h$$

and following arguments in the proof of Theorem 3.1 in [30], we can show the existence and uniqueness of Problem 3.2.

Proposition 3.4. *Assume $\alpha_* m > \alpha_j c_j^2$. Then the solution $u^h \in K^h$ of Problem 3.2 is uniformly bounded independent of h.*

Proof. We let $v^h = 0$ in (3.8) to get

$$a^h(u^h, u^h) \le j^0(\gamma_j u^h; -\gamma_j u^h) + \langle f^h, u^h\rangle. \tag{3.9}$$

From (2.8), (2.7) and (2.4),

$$\begin{aligned} j^0(\gamma_j u^h; -\gamma_j u^h) &\le \alpha_j \|\gamma_j u^h\|_{V_j}^2 - j^0(0; \gamma_j u^h) \\ &\le \alpha_j \|\gamma_j u^h\|_{V_j}^2 + c_0 \|\gamma_j u^h\|_{V_j} \\ &\le \alpha_j c_j^2 \|u^h\|_V^2 + c\|u^h\|_V. \end{aligned} \tag{3.10}$$

Also, $\langle f^h, u^h\rangle \le \|f^h\|_{(V^h)^*} \|u^h\|_V$ and recall that $\|f^h\|_{(V^h)^*}$ is uniformly bounded. Apply (2.5), (3.6) and (3.10) in (3.9),

$$\left(\alpha_* m - \alpha_j c_j^2\right) \|u^h\|_V^2 \le c\|u^h\|_V.$$

We then conclude that $u^h \in K^h$ is uniformly bounded independent of h. ■

In the following theorem, we present a general Céa's inequality that will be the starting point for deriving convergence order error estimates of the virtual element scheme (3.8) for solving the hemivariational inequality (2.3).

Theorem 3.5. *Assume $\alpha_* m > \alpha_j c_j^2$. Let u and u^h be the solutions of Problems 2.3 and 3.2, respectively. For any approximation $u^I \in K^h$ of u and for any piecewise polynomial approximation u^π of u, i.e. $u^\pi|_T \in \mathbb{P}^k(T)$ for all $T \in \mathcal{T}^h$, we have*

$$\|u - u^h\|_V \le c\left(\|u - u^I\|_V + \|u - u^\pi\|_{V,h} + \|f - f^h\|_{(V^h)^*} + \|\gamma_j u - \gamma_j u^I\|_{V_j}^{1/2} + |Re|^{1/2}\right), \tag{3.11}$$

where the constant c depends only on α, M, α_* and α^*. Here,

$$\|f - f^h\|_{(V^h)^*} := \sup_{v^h \in V^h} \frac{\langle f, v^h\rangle - \langle f^h, v^h\rangle}{\|v^h\|_V},$$

and

$$Re := a(u, e^h) - j^0(\gamma_j u; -\gamma_j e^h) - \langle f, e^h\rangle.$$

Proof. First, we split the error $e = u - u^h$ into two parts:

$$e = e^I + e^h,$$

where

$$e^I := u - u^I, \quad e^h := u^I - u^h.$$

From (2.5) and (3.6),

$$\alpha_* m \|e^h\|_V^2 \le \alpha_* a(e^h, e^h) \le a^h(e^h, e^h) = a^h(u^I, e^h) - a^h(u^h, e^h).$$

By (3.8),

$$\alpha_* m \|e^h\|_V^2 \le a^h(u^I, e^h) - \langle f^h, e^h\rangle + j^0(\gamma_j u^h; \gamma_j e^h).$$

Applying (3.3), we rewrite the right hand side of the above inequality:

$$\begin{aligned}\alpha_* m \|e^h\|_V^2 &\le \sum_T \left(a_T^h(u^I - u^\pi, e^h) + a_T^h(u^\pi, e^h)\right) - \langle f^h, e^h\rangle + j^0(\gamma_j u^h; \gamma_j e^h)\\ &= \sum_T \left(a_T^h(u^I - u^\pi, e^h) + a_T(u^\pi, e^h)\right) - \langle f^h, e^h\rangle + j^0(\gamma_j u^h; \gamma_j e^h)\\ &= \sum_T \left(a_T^h(u^I - u^\pi, e^h) + a_T(u^\pi - u, e^h)\right) + a(u, e^h) - \langle f^h, e^h\rangle + j^0(\gamma_j u^h; \gamma_j e^h),\end{aligned}$$

i.e.,

$$\alpha_* m \|e^h\|_V^2 \le R_1 + R_2 + R_3 + Re, \tag{3.12}$$

where

$$\begin{aligned}R_1 &= \sum_T \left(a_T^h(u^I - u^\pi, e^h) + a_T(u^\pi - u, e^h)\right),\\ R_2 &= \langle f, e^h\rangle - \langle f^h, e^h\rangle,\\ R_3 &= j^0(\gamma_j u^h; \gamma_j e^h) + j^0(\gamma_j u; -\gamma_j e^h),\\ Re &= a(u, e^h) - j^0(\gamma_j u; -\gamma_j e^h) - \langle f, e^h\rangle.\end{aligned}$$

Next, we bound the first three terms on the right side of (3.12). By (2.6) and (3.5), we get

$$R_1 \le \alpha^* M \|u^I - u^\pi\|_{V,h} \|e^h\|_V + M\|u^\pi - u\|_{V,h}\|e^h\|_V. \tag{3.13}$$

In addition,

$$R_2 \le \|f - f^h\|_{(V^h)^*}\|e^h\|_V. \tag{3.14}$$

Applying the properties (2.2), (2.7) and (2.8), we have

$$\begin{aligned}R_3 &= j^0(\gamma_j u^h; \gamma_j u^I - \gamma_j u^h) + j^0(\gamma_j u; \gamma_j u^h - \gamma_j u^I)\\ &\le j^0(\gamma_j u^h; \gamma_j u^I - \gamma_j u) + j^0(\gamma_j u^h; \gamma_j u - \gamma_j u^h)\\ &\quad + j^0(\gamma_j u; \gamma_j u^h - \gamma_j u) + j^0(\gamma_j u; \gamma_j u - \gamma_j u^I)\\ &\le (c_0 + c_1\|\gamma_j u^h\|_{V_j})\|\gamma_j u - \gamma_j u^I\|_{V_j} + \alpha_j\|\gamma_j u - \gamma_j u^h\|_{V_j}^2\\ &\quad + (c_0 + c_1\|\gamma_j u\|_{V_j})\|\gamma_j u - \gamma_j u^I\|_{V_j}.\end{aligned}$$

By Proposition 3.4, $\|u^h\|_V$ is uniformly bounded independent of h. Hence, by (2.4), we have

$$R_3 \le \alpha_j c_j^2 \|u - u^h\|_V^2 + c\|\gamma_j u - \gamma_j u^I\|_{V_j}. \tag{3.15}$$

Combining (3.12)–(3.15), we have

$$\begin{aligned}\|e^h\|_V^2 \le{}& \frac{1}{\alpha_* m}\left(\alpha^* M\|u^I - u^\pi\|_{V,h} + M\|u^\pi - u\|_{V,h} + \|f - f^h\|_{(V^h)^*}\right)\|e^h\|_V\\ &+ \frac{\alpha_j c_j^2}{\alpha_* m}\|u - u^h\|_V^2 + c\left(\|\gamma_j u - \gamma_j u^I\|_{V_j} + |Re|\right).\end{aligned} \tag{3.16}$$

Note that if $x^2 \le ax + b$ and $x > 0$, $a > 0$, $b > 0$, we have $x \le a + b^{1/2}$. Thus,

$$\begin{aligned}\|e^h\|_V \le{}& \frac{1}{\alpha_* m}\left(\alpha^* M\|u^I - u^\pi\|_{V,h} + M\|u^\pi - u\|_{V,h} + \|f - f^h\|_{(V^h)^*}\right)\\ &+ \left(\frac{\alpha_j c_j^2}{\alpha_* m}\|u - u^h\|_V^2 + c\left(\|\gamma_j u - \gamma_j u^I\|_{V_j} + |Re|\right)\right)^{1/2}.\end{aligned} \tag{3.17}$$

Finally, the proof is completed by the triangle inequality

$$\|u - u^h\|_V \le \|u - u^I\|_V + \|u^I - u^h\|_V$$

with the assumption that $\alpha_* m > \alpha_j c_j^2$. ∎

3.3. Virtual element scheme for HVI without constraint

For the special case that $K = V$, we have $K^h = V^h$, then Problem 2.3 and its virtual element approximation (3.8) become

$$a(u, v) + j^0(\gamma_j u; \gamma_j v) \geq \langle f, v\rangle \quad \forall\, v \in V, \tag{3.18}$$

and

$$a^h(u^h, v^h) + j^0(\gamma_j u^h; \gamma_j v^h) \geq \langle f^h, v^h\rangle \quad \forall\, v^h \in V^h. \tag{3.19}$$

By an argument similar to that of the proof in Theorem 3.5, we can derive same result that

$$\alpha_* m\|e^h\|_V^2 \leq R_1 + R_2 + R_3 + Re.$$

To bound the terms R_1, R_2 and R_3, we use the same arguments in Theorem 3.5. Let us consider the residual term Re. Because $-e^h \in V$, by (3.18), we have

$$a(u, -e^h) + j^0(\gamma_j u; -\gamma_j e^h) \geq \langle f, -e^h\rangle \quad \forall\, v \in V.$$

Hence,

$$\begin{aligned} Re &= a(u, e^h) - j^0(\gamma_j u; -\gamma_j e^h) - \langle f, e^h\rangle \\ &\leq a(u, e^h) + a(u, -e^h) - \langle f, -e^h\rangle - \langle f, e^h\rangle \\ &= 0. \end{aligned}$$

Then the general estimation (3.11) reduces to

$$\|u - u^h\|_V \leq c\left(\|u - u^I\|_V + \|u - u^\pi\|_{V,h} + \|f - f^h\|_{(V^h)^*} + \|\gamma_j u - \gamma_j u^I\|_{V_j}^{1/2}\right). \tag{3.20}$$

The above inequality and Theorem 3.5 are starting points for the error estimation for specific elliptic hemivariational inequalities arising in contact problems discussed in Section 2.3.

4. Construction of the VEM

To make this paper self-contained, following [19,23], we present ideas for construction of the virtual element space $V^h \subset V$, the corresponding bilinear form a^h and the right-hand side f^h satisfying Assumption 3.1.

For simplicity, we only consider two-dimensional case in the rest of the paper. Assume Ω is a polygonal domain and express the three parts of the boundary, Γ_k, $1 \leq k \leq 3$, as unions of closed line segments with disjoint interiors:

$$\overline{\Gamma_k} = \cup_{i=1}^{i_k} \Gamma_{k,i}, \quad 1 \leq k \leq 3.$$

Let $\{\mathcal{T}^h\}$ be a family of partitions of $\overline{\Omega}$ into elements T that are compatible with the partition of the boundary $\partial\Omega$ into $\Gamma_{k,i}$, $1 \leq i \leq i_k$, $1 \leq k \leq 3$, in the sense that if one side $e \subset \partial T$ satisfies $\text{meas}(e \cap \Gamma_{k,i}) > 0$, then $e \subset \Gamma_{k,i}$. Let $\mathcal{E}^h$ stand for the set of all the edges of $\mathcal{T}^h$, and let $\mathcal{E}_i^h$ be the set of all the interior edges. Denote by $\mathcal{E}_1^h$, $\mathcal{E}_2^h$ and $\mathcal{E}_3^h$ the set of all the edges lie on Γ_1, Γ_2 and Γ_3, respectively. Let $\mathcal{E}_0^h = \mathcal{E}_i^h \cup \mathcal{E}_2^h \cup \mathcal{E}_3^h$ be the set of all the edges that do not lie on Γ_1. Denote $\mathcal{P}_0^h$ as the set of all the vertices that do not lie on Γ_1. Set $h_T = \text{diam}(T)$ and $h = \max\{h_T : T \in \mathcal{T}^h\}$.

As in [18,19,31], we make the following assumption.

Assumption 4.1. There exists a constant number $\delta > 0$ such that for each h and every $T \in \mathcal{T}^h$,

- T is star-shaped with respect to a ball of radius δh_T;
- The distance between any two vertices of T is greater than or equal to δh_T.

4.1. Construction of the virtual element space

Let T be a polygon with n edges. For $k \geq 1$, we define the local finite dimensional space W_T^h on the element T,

$$W_T^h := \{\boldsymbol{v} \in H^1(T;\mathbb{R}^2) : \nabla\cdot\mathcal{C}\boldsymbol{\varepsilon}(\boldsymbol{v}) \in \mathbb{P}_{k-2}(T;\mathbb{R}^2),\ \boldsymbol{v}|_{\partial T} \in C^0(\partial T),\ \boldsymbol{v}|_e \in \mathbb{P}_k(e;\mathbb{R}^2)\ \forall\, e \subset \partial T\} \tag{4.1}$$

with the convention that $\mathbb{P}_{-1}(T) = \{0\}$. For a function $\boldsymbol{v} \in W_T^h$, we choose the following degrees of freedom:

- The values of $\boldsymbol{v}(\boldsymbol{a})$ $\quad\forall$ vertex $\boldsymbol{a} \in T$, (4.2)
- The moments $\displaystyle\int_e \boldsymbol{q}\cdot\boldsymbol{v}\,ds \quad \forall\, q \in \mathbb{P}_{k-2}(e;\mathbb{R}^2) \quad \forall$ edge $e \subset \partial T$, $\quad k \geq 2$, (4.3)
- The moments $\displaystyle\int_T \boldsymbol{q}\cdot\boldsymbol{v}\,dx \quad \forall\, q \in \mathbb{P}_{k-2}(T;\mathbb{R}^2)$, $\quad k \geq 2$. (4.4)

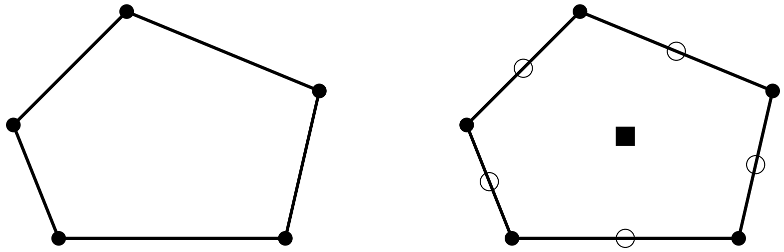

Fig. 1. Local d.o.f. of the virtual element for $k = 1$ (left) and $k = 2$ (right).

In Fig. 1, we show the degrees of freedom for the first two low-order elements with $k = 1$ and $k = 2$. It is easy to check that the degree of freedom corresponding to T is

$$N^T_{\text{dof}} = 2nk + k(k-1).$$

For every decomposition $\mathcal{T}^h$ and $k \geq 1$, define the global virtual element space W^h as

$$W^h := \{\boldsymbol{v} \in W : \boldsymbol{v}|_T \in W^h_T \quad \forall T \in \mathcal{T}^h\}, \tag{4.5}$$

and the global degrees of freedom for $\boldsymbol{v} \in W^h$ can then be taken as

- The values of $\boldsymbol{v}(\boldsymbol{a}) \quad \forall \text{vertex } \boldsymbol{a} \in \mathcal{P}^h_0$, (4.6)
- The moments $\int_e \boldsymbol{q} \cdot \boldsymbol{v}\, ds \quad \forall \boldsymbol{q} \in \mathbb{P}_{k-2}(e; \mathbb{R}^2) \quad \forall \text{edge } e \in \mathcal{E}^h_0,\ k \geq 2$, (4.7)
- The moments $\int_T \boldsymbol{q} \cdot \boldsymbol{v}\, dx \quad \forall \boldsymbol{q} \in \mathbb{P}_{k-2}(T; \mathbb{R}^2) \quad \forall \text{element } T \in \mathcal{T}^h,\ k \geq 2$. (4.8)

The dimension of W^h coincides with the total number of degrees of freedom (4.6)–(4.8), which is given by

$$N_{\text{dof}} = 2N_V + 2(k-1)N_E + k(k-1)N_T,$$

where N_V is the number of vertices in $\mathcal{P}^h_0$, N_E is the number of edges in $\mathcal{E}^h_0$, and N_T is the number of elements. It was proved in [19] that the degrees of freedom (4.6)–(4.8) are unisolvent for W^h.

Denote by χ_i the ith degree of freedom for W^h, $i = 1, 2, \ldots, N_{\text{dof}}$. From the above construction, it follows that for every sufficiently smooth function $\boldsymbol{w}$, there exists a unique element $\boldsymbol{w}^I \in W^h$ such that

$$\chi_i(\boldsymbol{w} - \boldsymbol{w}^I) = 0, \quad i = 1, 2, \ldots, N_{\text{dof}}.$$

Then by the scaling argument and Bramble–Hilbert Lemma, the following approximation property holds [19]

$$\|\boldsymbol{w} - \boldsymbol{w}^I\|_{t,\Omega} \leq Ch^{s-t}|\boldsymbol{w}|_{s,\Omega}, \quad t = 0, 1,\ 2 \leq s \leq k+1. \tag{4.9}$$

Furthermore, for every $T \in \mathcal{T}^h$ and every $\boldsymbol{w} \in H^s(T; \mathbb{R}^2)$, there exists a function $\boldsymbol{w}^\pi \in \mathbb{P}_k(T; \mathbb{R}^2)$ such that [19,32]

$$\|\boldsymbol{w} - \boldsymbol{w}^\pi\|_{t,T} \leq Ch_T^{s-t}|\boldsymbol{w}|_{s,T}, \quad t = 0, 1, \quad 1 \leq s \leq k+1. \tag{4.10}$$

4.2. Construction of a^h

Using the ideas in [19,23], we now present a symmetric and computable discrete bilinear form a^h satisfying Assumption 3.1.

In order to construct $a^h(\cdot,\cdot)$, we first define a projection operator $\Pi^T_k : W^h_T \to \mathbb{P}_k(T; \mathbb{R}^2)$ by

$$a_T(\Pi^T_k \boldsymbol{v}^h, \boldsymbol{q}) = a_T(\boldsymbol{v}^h, \boldsymbol{q}) \quad \forall \boldsymbol{q} \in \mathbb{P}_k(T; \mathbb{R}^2). \tag{4.11}$$

This equation determines $\Pi^T_k \boldsymbol{v}^h$ only up to a rigid motion. In order to ensure the uniqueness, we adopt the idea in [23] to use the following conditions

$$\frac{1}{n^T_V}\sum_{i=1}^{n^T_V} \Pi^T_k \boldsymbol{v}^h(\boldsymbol{x}_i) = \frac{1}{n^T_V}\sum_{i=1}^{n^T_V} \boldsymbol{v}^h(\boldsymbol{x}_i),$$
$$\frac{1}{n^T_V}\sum_{i=1}^{n^T_V} \boldsymbol{x}_i \times \Pi^T_k \boldsymbol{v}^h(\boldsymbol{x}_i) = \frac{1}{n^T_V}\sum_{i=1}^{n^T_V} \boldsymbol{x}_i \times \boldsymbol{v}^h(\boldsymbol{x}_i),$$

where $\boldsymbol{x}_i$ are the coordinates of the vertices of the element T and n^T_V denotes the number of the vertices. Here, "$\times$" denotes the cross product of two vectors.

Then we define the local bilinear form

$$a_T^h(\boldsymbol{u}^h, \boldsymbol{v}^h) := a_T(\Pi_k^T \boldsymbol{u}^h, \Pi_k^T \boldsymbol{v}^h) + S_T\left((I - \Pi_k^T)\boldsymbol{u}^h, (I - \Pi_k^T)\boldsymbol{v}^h\right) \quad \forall\, \boldsymbol{u}^h, \boldsymbol{v}^h \in W_T^h, \tag{4.12}$$

where

$$S_T(\boldsymbol{u}^h, \boldsymbol{v}^h) = \sum_{i=1}^{N_T^{\rm dof}} \chi_i(\boldsymbol{u}^h)\, \chi_i(\boldsymbol{v}^h)$$

is the stabilization term. The construction of $a^h(\boldsymbol{u}^h, \boldsymbol{v}^h) = \sum_{T\in\mathcal{T}^h} a_T^h(\boldsymbol{u}^h, \boldsymbol{v}^h)$ ensures the properties (3.3) and (3.4). Note that the bilinear form a^h can be constructed in other ways to guarantee the properties (3.3) and (3.4), for example, the construction of the bilinear form proposed in [21], which is adopted in [28].

4.3. Construction of the right-hand side $\boldsymbol{f}^h$

Note that the first term $(\boldsymbol{f}_1, \boldsymbol{v})_{L^2(\Omega;\mathbb{R}^2)}$ in (2.16) is not computable for $\boldsymbol{v} \in W^h$. Therefore, for $k \geq 2$, let

$$\boldsymbol{f}_{1T}^h = P_{k-2}^T \boldsymbol{f}_1 \quad \forall\, T \in \mathcal{T}^h,$$

i.e. on each element T, $\boldsymbol{f}_{1T}^h$ is the L^2-projection of $\boldsymbol{f}_1$ onto the space of polynomials of order $k-2$. Then we define

$$\langle \boldsymbol{f}_1^h, \boldsymbol{v}^h\rangle = \sum_{T\in\mathcal{T}^h} \int_T \boldsymbol{f}_{1T}^h \cdot \boldsymbol{v}^h\, dx \quad \forall\, \boldsymbol{v}^h \in W^h.$$

For $k = 1$, we choose

$$\boldsymbol{f}_{1T}^h = P_0^T \boldsymbol{f}_1 \quad \forall\, T \in \mathcal{T}^h$$

and define

$$\langle \boldsymbol{f}_1^h, \boldsymbol{v}^h\rangle = \sum_{T\in\mathcal{T}^h} \int_T \boldsymbol{f}_{1T}^h \cdot \overline{\boldsymbol{v}^h}\, dx \quad \forall\, \boldsymbol{v}^h \in W^h.$$

Here, $\overline{\boldsymbol{v}^h}$ denotes the average value of the function $\boldsymbol{v}^h$ over all vertices of T.

Finally, to approximate the right-hand side term $\langle \boldsymbol{f}, \boldsymbol{v}\rangle_{W^*\times W}$, we set

$$\langle \boldsymbol{f}^h, \boldsymbol{v}^h\rangle = \langle \boldsymbol{f}_1^h, \boldsymbol{v}^h\rangle + (\boldsymbol{f}_2, \boldsymbol{v}^h)_{L^2(\Gamma_2;\mathbb{R}^2)} \quad \forall\, \boldsymbol{v} \in W^h.$$

Then the following approximation property holds [19]

$$\|\boldsymbol{f} - \boldsymbol{f}^h\|_{(W^h)^*} \leq C\, h^k |\boldsymbol{f}|_{k-1}, \tag{4.13}$$

which ensures the optimal error bound.

5. Error analysis for contact problems

We illustrate applications of the framework developed in Section 3 on error estimation for the virtual element solutions of the three static contact problems.

5.1. VEM for Problem (P_1)

The function space corresponding to the virtual element method:

$$V^h = \left\{\boldsymbol{v}^h \in W^h : v_\nu^h = 0 \text{ on } \Gamma_3\right\}. \tag{5.1}$$

The virtual element scheme for Problem (P_1) is the following:

Problem (P_1^h). Find a displacement field $\boldsymbol{u}^h \in V^h$ such that

$$a^h(\boldsymbol{u}^h, \boldsymbol{v}^h) + \int_{\Gamma_3} j_\tau^0(\boldsymbol{u}_\tau^h; \boldsymbol{v}_\tau^h)\, ds \geq \langle \boldsymbol{f}^h, \boldsymbol{v}^h\rangle \quad \forall\, \boldsymbol{v}^h \in V^h. \tag{5.2}$$

Note that the discussion and result from Section 3 are still valid with $j^0(\gamma_j u, \gamma_j v)$ replaced by $\int_{\Gamma_3} j_\tau^0(\boldsymbol{u}_\tau; \boldsymbol{v}_\tau)\, ds$. Under Assumption 2.4, Problem (P_1^h) has a unique solution $\boldsymbol{u}^h \in V^h$. The conditions (2.5)–(2.6) follow from (2.14)(a)–(b). By applying the estimation (3.20), we have

$$\|\boldsymbol{u} - \boldsymbol{u}^h\|_V \leq c\left(\|\boldsymbol{u} - \boldsymbol{u}^I\|_V + \|\boldsymbol{u} - \boldsymbol{u}^\pi\|_{V,h} + \|\boldsymbol{f} - \boldsymbol{f}^h\|_{(V^h)^*} + \|\boldsymbol{u}_\tau - \boldsymbol{u}_\tau^I\|_{L^2(\Gamma_3;\mathbb{R}^2)}^{1/2}\right). \tag{5.3}$$

Then we conclude the optimal order error bound for $k = 1$,

$$\|\boldsymbol{u} - \boldsymbol{u}^h\|_V \le c\, h \tag{5.4}$$

under the regularity assumptions

$$\boldsymbol{u} \in H^2(\Omega; \mathbb{R}^2), \quad \boldsymbol{u}_\tau \in H^2(\Gamma_{3,i}; \mathbb{R}^2),\ 1 \le i \le i_3. \tag{5.5}$$

5.2. VEM for Problem (P_2)

We use the virtual element space $V^h = W^h$ of (4.5) and introduce the following approximation of Problem (P_2).

Problem (P_2^h). Find a displacement field $\boldsymbol{u}^h \in V^h$ such that

$$a^h(\boldsymbol{u}^h, \boldsymbol{v}^h) + \int_{\Gamma_3} j_\nu^0(u_\nu^h; v_\nu^h)\, ds \ge \langle \boldsymbol{f}^h, \boldsymbol{v}^h\rangle \quad \forall\, \boldsymbol{v}^h \in V^h. \tag{5.6}$$

The discussion and result from Section 3 are still valid with $j^0(\gamma_j u, \gamma_j v)$ replaced by $\int_{\Gamma_3} j_\nu^0(u_\nu^h; v_\nu^h)\, ds$. From the error estimate (3.20), we obtain

$$\|\boldsymbol{u} - \boldsymbol{u}^h\|_V \le c \left(\|\boldsymbol{u} - \boldsymbol{u}^I\|_V + \|\boldsymbol{u} - \boldsymbol{u}^\pi\|_{V,h} + \|\boldsymbol{f} - \boldsymbol{f}^h\|_{(V^h)^*} + \|u_\nu - u_\nu^I\|_{L^2(\Gamma_3)}^{1/2} \right). \tag{5.7}$$

Moreover, under the regularity assumptions

$$\boldsymbol{u} \in H^2(\Omega; \mathbb{R}^2), \quad u_\nu \in H^2(\Gamma_{3,i}),\ 1 \le i \le i_3, \tag{5.8}$$

we have the optimal order error bound for $k = 1$

$$\|\boldsymbol{u} - \boldsymbol{u}^h\|_V \le c\, h. \tag{5.9}$$

Remark 5.1. Note that we cannot derive optimal order error estimate from (5.3) and (5.7) for higher order virtual elements. For example, if we set $k = 2$ in defining the virtual element space V^h, we can only get a sub-optimal error estimate

$$\|\boldsymbol{u} - \boldsymbol{u}^h\|_V \le c\, h^{3/2}.$$

even under higher solution regularity assumptions

$$\boldsymbol{u} \in H^3(\Omega; \mathbb{R}^2), \quad \boldsymbol{u}_\tau \in H^3(\Gamma_{3,i}; \mathbb{R}^2),\ 1 \le i \le i_3,$$

or

$$\boldsymbol{u} \in H^3(\Omega; \mathbb{R}^2), \quad u_\nu \in H^3(\Gamma_{3,i}),\ 1 \le i \le i_3,$$

due to the error bound terms on the contact boundary Γ_3. However, if we refine the elements along Γ_3 several times such that $h_3 = O(h^{\frac{4}{3}})$ ($h_3 = \max\{h_e : e \in \mathcal{E}_3^h\}$), the optimal convergence order can be achieved with respect to the degrees of freedom. See Fig. 2 for a local refined mesh along the contact boundary $\Gamma_3 = [0, L] \times \{0\}$. We know that such meshes can be easily obtained with the virtual element framework since the hanging nodes are allowed, which is one advantage of VEM for solving contact problems.

5.3. VEM for Problem (P_3)

To approximate the admissible set U, let us use a related function subset of the virtual element space $V^h = W^h$ with $k = 1$ defined in (4.5):

$$U^h = \left\{ \boldsymbol{v}^h \in V^h : v_\nu^h \le g \text{ at node points on } \Gamma_3 \right\}. \tag{5.10}$$

Assume g is a concave function. Then $U^h \subset U$. We define the following numerical method for Problem (P_3).

Problem (P_3^h). Find a displacement field $\boldsymbol{u}^h \in U^h$ such that

$$a^h(\boldsymbol{u}^h, \boldsymbol{v}^h - \boldsymbol{u}^h) + \int_{\Gamma_3} j_\nu^0(u_\nu^h; v_\nu^h - u_\nu^h)\, ds \ge \langle \boldsymbol{f}^h, \boldsymbol{v}^h - \boldsymbol{u}^h\rangle \quad \forall\, \boldsymbol{v}^h \in U^h. \tag{5.11}$$

Note that the discussion and result from Section 3 are still valid with $j^0(\gamma_j u, \gamma_j v)$ replaced by $\int_{\Gamma_3} j_\nu^0(u_\nu^h; v_\nu^h)\, ds$, with the quantity Re modified as

$$Re = a(\boldsymbol{u}, \boldsymbol{e}^h) - \int_{\Gamma_3} j_\nu^0(u_\nu; -e_\nu^h)\, ds - \langle \boldsymbol{f}, \boldsymbol{e}^h\rangle.$$

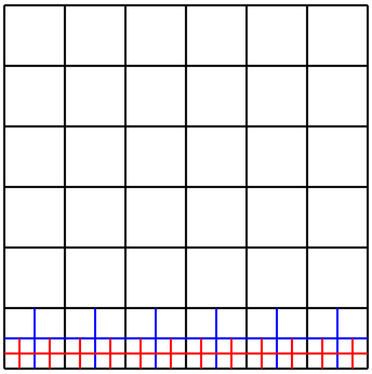

Fig. 2. A local refined mesh along $\Gamma_3 = [0, L] \times \{0\}$.

We apply Theorem 3.5 to derive an error estimate. The key step is to bound the residual term $|Re|^{1/2}$. With the regularity assumption (5.8), we can deduce the following relations:

$$-\nabla \cdot \boldsymbol{\sigma} = \boldsymbol{f}_1 \quad \text{a.e. in } \Omega, \tag{5.12}$$

$$\boldsymbol{\sigma}\boldsymbol{\nu} = \boldsymbol{f}_2 \quad \text{a.e. on } \Gamma_2, \tag{5.13}$$

$$\boldsymbol{\sigma}_\tau = \boldsymbol{0} \quad \text{a.e. on } \Gamma_3, \tag{5.14}$$

$$\int_{\Gamma_3} \sigma_\nu (v_\nu - u_\nu)\, ds + \int_{\Gamma_3} j_\nu^0(u_\nu; v_\nu - u_\nu)\, ds \ge 0 \quad \forall\, \boldsymbol{v} \in U. \tag{5.15}$$

by the argument similar to that in [33, Section 8.1]. We write

$$\begin{aligned} Re &= \int_\Omega (-\nabla \cdot \boldsymbol{\sigma}) \cdot \boldsymbol{e}^h\, dx + \int_\Gamma (\boldsymbol{\sigma}\boldsymbol{\nu}) \cdot \boldsymbol{e}^h\, ds - \int_{\Gamma_3} j_\nu^0(u_\nu; -e_\nu^h)\, ds - \langle \boldsymbol{f}, \boldsymbol{e}^h \rangle \\ &= \int_{\Gamma_3} \sigma_\nu (u_\nu^I - u_\nu^h)\, ds - \int_{\Gamma_3} j_\nu^0(u_\nu; u_\nu^h - u_\nu^I)\, ds \\ &= \int_{\Gamma_3} \sigma_\nu (u_\nu^I - u_\nu)\, ds + \int_{\Gamma_3} \sigma_\nu (u_\nu - u_\nu^h)\, ds - \int_{\Gamma_3} j_\nu^0(u_\nu; u_\nu^h - u_\nu)\, ds \\ &\quad + \int_{\Gamma_3} j_\nu^0(u_\nu; u_\nu^h - u_\nu)\, ds - \int_{\Gamma_3} j_\nu^0(u_\nu; u_\nu^h - u_\nu^I)\, ds. \end{aligned}$$

Note that $\boldsymbol{u}^h \in U$, and by (5.15),

$$\int_{\Gamma_3} \sigma_\nu (u_\nu - u_\nu^h)\, ds - \int_{\Gamma_3} j_\nu^0(u_\nu; u_\nu^h - u_\nu)\, ds \le 0.$$

Hence,

$$\begin{aligned} Re &\le \int_{\Gamma_3} \sigma_\nu (u_\nu^I - u_\nu)\, ds + \int_{\Gamma_3} j_\nu^0(u_\nu; u_\nu^h - u_\nu)\, ds - \int_{\Gamma_3} j_\nu^0(u_\nu; u_\nu^h - u_\nu^I)\, ds \\ &= \int_{\Gamma_3} \sigma_\nu (u_\nu^I - u_\nu)\, ds + \int_{\Gamma_3} j_\nu^0(u_\nu; u_\nu^I - u_\nu)\, ds \\ &\le c \|u_\nu - u_\nu^I\|_{L^2(\Gamma_3)} \end{aligned}$$

by the subadditivity (2.2). Then

$$|Re|^{1/2} \le c^{1/2} \|u_\nu - u_\nu^I\|_{L^2(\Gamma_3)}^{1/2}.$$

Recalling the solution regularity (5.8), an assumption made earlier in order to derive the pointwise equations (5.12) and (5.14), we conclude the optimal order error bound for $k = 1$,

$$\|\boldsymbol{u} - \boldsymbol{u}^h\|_V \le c\, h.$$

Remark 5.2.

1. In this paper, we only consider the 2-dimensional virtual element method for solving the hemivariational inequalities and derive error estimates. For the 3-dimensional case, we may follow the ideas presented in [20,34,35] to

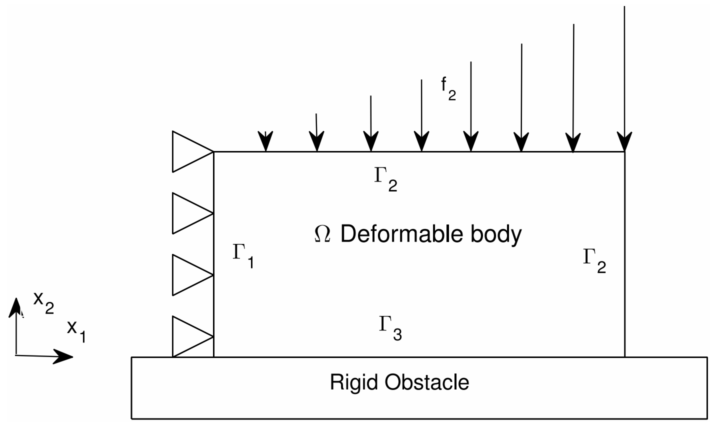

Fig. 3. Physical configuration for Example 6.1.

construct the virtual element method for solving these problems. However, development and analysis of virtual element methods to solve the 3-dimensional contact problems are more complicated and further studies are needed.

2. Compared with conforming VEM, the lowest-order nonconforming VEM [22] can avoid locking phenomena for solving nearly incompressible elasticity problems. The analysis in this paper can be extended to the nonconforming VEM, as did in [36], and it is worth studying in the future.

6. Numerical examples

In this section, we report numerical results on the lowest order VEM for the elliptic HVI problems. To solve the discretized problems, the Lagrange multiplier [37] approach and the convexification iteration method [38–40] can be used.

In the following examples, the elasticity tensor $\mathcal{C}$ satisfies

$$\sigma_{ij} = (\mathcal{C}\boldsymbol{\varepsilon})_{ij} = \frac{E\kappa}{1-\kappa^2}(\varepsilon_{11}+\varepsilon_{22})\delta_{ij} + \frac{E}{1+\kappa}\varepsilon_{ij}, \quad 1 \le i, j \le 2,$$

where E is the Young modulus, κ is the Poisson ratio of the material and $\delta_{\alpha,\beta}$ denotes the Kronecker symbol.

First, let us consider an example of Problem (P_1), the bilateral contact problem with friction. A similar example was reported in [39] using the finite element method.

Example 6.1. Let $\Omega = (0, L_1)\times(0, L_2)$ with its boundary Γ divided into three subsets: $\Gamma_1 = \{0\}\times[0, L_2]$, $\Gamma_3 = [0, L_1]\times\{0\}$, $\Gamma_2 = \Gamma\backslash(\Gamma_1 \cup \Gamma_3)$. No body force acts on Ω. On Γ_1, the elastic body is clamped, and therefore, the displacement field vanishes there. Vertical traction acts on the boundary $[0, L_1] \times \{L_2\}$, and it is traction free on $\{L_1\} \times [0, L_2]$. The body is in bilateral frictional contact with a rigid foundation on Γ_3. The physical setting is depicted in Fig. 3.

The friction is modeled by a nonmonotone law in which the friction coefficient μ depends on the tangential displacement $|\boldsymbol{u}_\tau|$. Let us consider the following friction bound function

$$\mu(|\boldsymbol{u}_\tau|) = (a-b)\cdot e^{-\alpha|\boldsymbol{u}_\tau|} + b,$$

with $a \ge b > 0$ and $\alpha > 0$. In the example, we take $a = 1.5$, $b = 0.5$ and $\alpha = 100$.

For the computation, we used the following data:

$$L_1 = 2\ \mathrm{m}, \quad L_2 = 1\ \mathrm{m}, \quad E = 1000\ \mathrm{N/m^2}, \quad \kappa = 0.3,$$
$$\boldsymbol{f}_0(\boldsymbol{x}) = (0, 0)\ \mathrm{N/m^2},$$
$$\boldsymbol{f}_2(\boldsymbol{x}) = \begin{cases} (0, 0)\ \mathrm{N/m} & \text{for } \boldsymbol{x} \in \{2\} \times [0, 1], \\ (0, -200x_1)\ \mathrm{N/m} & \text{for } \boldsymbol{x} \in [0, 2] \times \{1\}. \end{cases}$$

In the bilateral friction boundary condition (2.17), we choose

$$j_\tau(\boldsymbol{u}_\tau) = S\int_0^{|\boldsymbol{u}_\tau|}\mu(t)\,dt$$

with $S = 1$. Then, by the Clark subdifferential, we have

$$\partial j_\tau(\boldsymbol{u}_\tau)\begin{cases} \in \mu(0)B_1(\mathbf{0}), & \text{if } \boldsymbol{u}_\tau = \mathbf{0}, \\ = \mu(|\boldsymbol{u}_\tau|)\dfrac{\boldsymbol{u}_\tau}{|\boldsymbol{u}_\tau|}, & \text{if } \boldsymbol{u}_\tau \ne \mathbf{0}. \end{cases}$$

Here, $B_1(\mathbf{0})$ is the unit circle centered at the origin.

Table 1
Errors and numerical convergence orders of the lowest order VEM for Example 6.1.

h	2^{-2}	2^{-3}	2^{-4}	2^{-5}	2^{-6}
Errors	6.6520e−2	3.4214e−2	1.7752e−2	9.2284e−3	4.6945e−3
Convergence orders	–	0.95919	0.94661	0.94383	0.97511

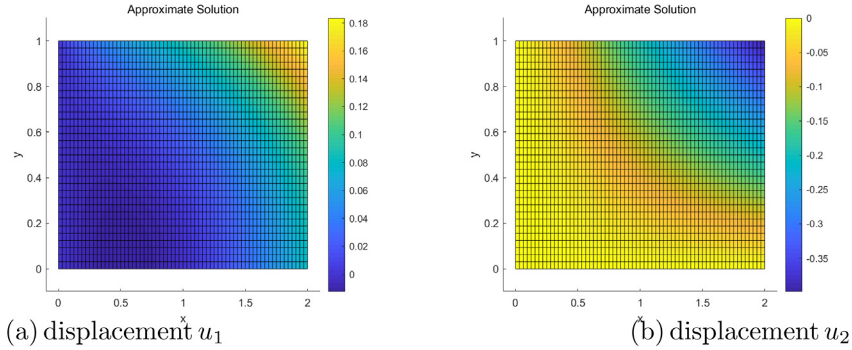

(a) displacement u_1 (b) displacement u_2

Fig. 4. Numerical solution for square mesh with $h = 2^{-5}$.

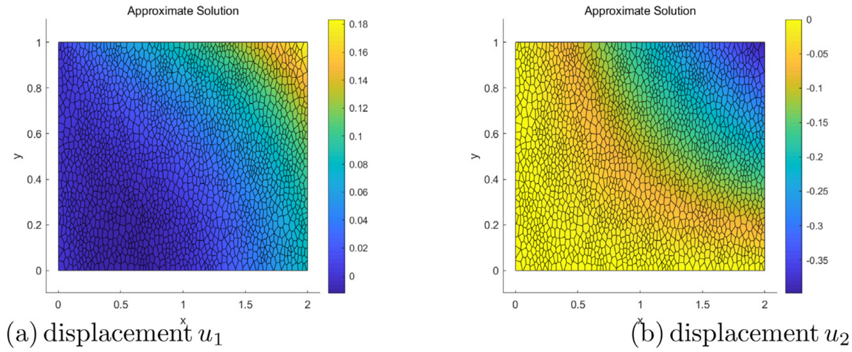

(a) displacement u_1 (b) displacement u_2

Fig. 5. Numerical solution for polygonal mesh of 2048 polygons.

To show the numerical convergence orders, we calculate the numerical solutions on a family of square meshes $\mathcal{T}^h$ with $h = 2^{-n}$, $n = 2, \ldots, 6$. Since the exact solution $\boldsymbol{u}$ is not available, we use the numerical solution corresponding to a fine mesh as the "reference" solution $\boldsymbol{u}_{ref}$ for computing the errors of the numerical solution $\boldsymbol{u}_h$. In Table 1, we report the H^1 error of the numerical solutions and the corresponding convergence orders. Because the virtual element solution $\boldsymbol{u}_h$ is not computable, instead, we compute the relative error $\left\|\Pi_1(\boldsymbol{u}_h - \boldsymbol{u}_{ref})\right\|_{H^1} / \left\|\Pi_1\boldsymbol{u}_{ref}\right\|_{H^1}$ with Π_1 is the projection defined by (4.11). Here, we use the numerical solution on the mesh $\mathcal{T}^h$ with $h = 2^{-8}$ as the "reference" solution $\boldsymbol{u}_{ref}$. We observe that the convergence is almost linear, which matches the theoretical expectation.

In Fig. 4, the components of the numerical solution $\boldsymbol{u}^h = (u_1, u_2)^T$ on square mesh with $h = 2^{-5}$ are displayed. In addition, the numerical solution on a polygonal mesh is shown in Fig. 5. Comparing these figures, we see that the numerical displacements are almost the same on both square and polygonal meshes.

Next, we consider an example of Problem (P_2), the normal compliance contact problem without friction. A similar example was reported in [41] using the finite element method.

Example 6.2. Let $\Omega = (0, L) \times (0, L)$, $\Gamma_2 = [0, L] \times \{L\}$, $\Gamma_3 = [0, L] \times \{0\}$, and $\Gamma_1 = \Gamma \backslash (\Gamma_2 \cup \Gamma_3)$. The physical setting is shown in Fig. 6. For the numerical simulation, we use

$$L = 1 \text{ m}, \quad E = 70 \text{ GPa}, \quad \kappa = 0.3,$$
$$\boldsymbol{f}_0(\boldsymbol{x}) = (0, 0) \text{ GPa}, \quad \boldsymbol{f}_2(\boldsymbol{x}) = \left(0, 32\,(x_1 - 0.5)^2 - 10\right) \text{ GPa m} \quad \text{on } \Gamma_2.$$

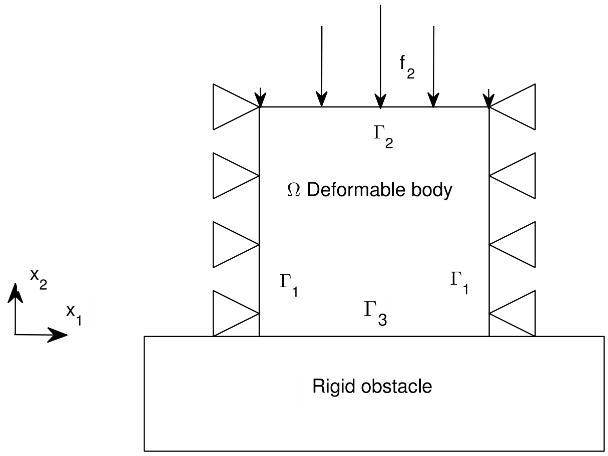

Fig. 6. Physical configuration for Example 6.2.

Table 2
Errors and numerical convergence orders for Example 6.2 ($\alpha = 120$).

h	2^{-2}	2^{-3}	2^{-4}	2^{-5}	2^{-6}
Errors	3.3734e−1	1.9093e−1	1.0308e−1	5.5144e−2	2.8661e−2
Convergence orders	–	0.82119	0.88926	0.90248	0.94413

Table 3
Errors and numerical convergence orders for Example 6.2 ($\alpha = 40$).

h	2^{-2}	2^{-3}	2^{-4}	2^{-5}	2^{-6}
Errors	3.3966e−1	1.9102e−1	1.0325e−1	5.5262e−2	2.8707e−2
Convergence orders	–	0.83036	0.88759	0.90178	0.94488

We consider a particular version of Problem (P_2), in which the contact condition (2.24) is given by $-\sigma_\nu = \xi_\nu(u_\nu)$ with

$$\xi_\nu(r) = \alpha(\beta r^+ + p(r)) \quad \text{and} \quad p(r) = \begin{cases} 0 & \text{if } r < 0, \\ r & \text{if } r \in [0, 0.01], \\ 0.02 - r & \text{if } r \in (0.01, 0.02], \\ r - 0.02 & \text{if } r > 0.02. \end{cases}$$

Here and below r^+ represents the positive part of r, i.e., $r^+ = max\{r, 0\}$, $\alpha > 0$ and $\beta > 0$ are the stiffness coefficients of the foundation.

Let $\beta = 0.5$, so the σ_ν is nonmonotone, and set $\alpha = 120$ or $\alpha = 40$. To show the convergence orders, we calculate the numerical solutions on a family of square meshes $\mathcal{T}^h$ with $h = 2^{-n}$, $n = 2, \ldots, 6$. In Tables 2 and 3, we list the relative errors $\left\| \Pi_1(\boldsymbol{u}^h - \boldsymbol{u}_{ref}) \right\|_{H^1} / \left\| \Pi_1 \boldsymbol{u}_{ref} \right\|_{H^1}$ and the convergence orders, which are around first order. Here, the "reference" solution $\boldsymbol{u}_{ref}$ is the numerical solution on the mesh $\mathcal{T}^h$ with $h = 2^{-8}$.

To observe the behaviors of the normal displacement u_ν and normal stress σ_ν on contact boundary Γ_3, we consider the numerical solution on mesh with $h = 2^{-6}$. For the case $\alpha = 120$, the normal displacement and normal stress on Γ_3 are plotted in Fig. 7; while the case with $\alpha = 40$ is shown in Fig. 8. In Fig. 7, we see that for $0 \le u_\nu < 0.01$ the normal force σ_ν increases with respect to u_ν, and for $0.01 \le u_\nu < 0.02$ the normal force decreases with respect to u_ν. In Fig. 8, we can divide the nodes as three parts: $0 \le u_\nu < 0.01$, $0.01 \le u_\nu < 0.02$, and $u_\nu \ge 0.02$. We observe that for $0 \le u_\nu < 0.01$ the normal force increases with respect to the penetration, for $0.01 \le u_\nu < 0.02$ it decreases, and the normal force increases when $u_\nu \ge 0.02$.

Finally, we consider an example of Problem (P_3), a frictionless contact with a foundation made of a rigid body covered by a layer made of elastic material. A similar example was reported in [41] using the finite element method.

Example 6.3. The basic physical setting (see Fig. 9) of this example is similar as Example 6.2, but the contact condition (2.29) is given by

$$u_\nu \le g, \quad \sigma_\nu + \xi_\nu(u_\nu) \le 0, \quad (u_\nu - g)(\sigma_\nu + \xi_\nu(u_\nu)) = 0$$

where

$$\xi_\nu(r) = \alpha(\beta r^+ + p(r))$$

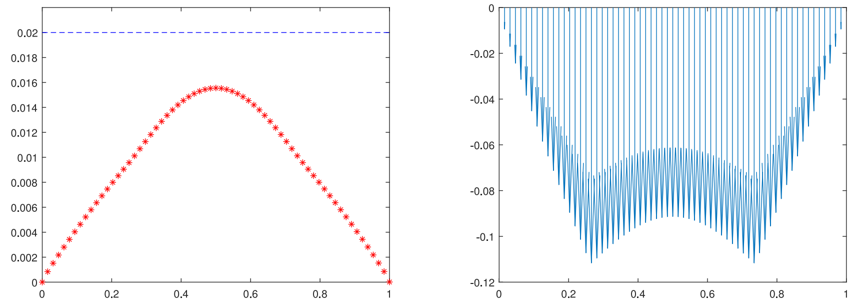

(a) normal displacement u_ν (b) normal stress σ_ν

Fig. 7. Normal displacement and normal stress with $\alpha = 120$ in Example 6.2.

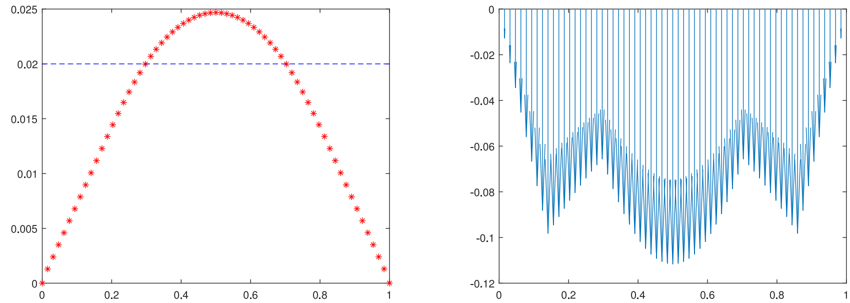

(a) normal displacement u_ν (b) normal stress σ_ν

Fig. 8. Normal displacement and normal stress with $\alpha = 40$ in Example 6.2.

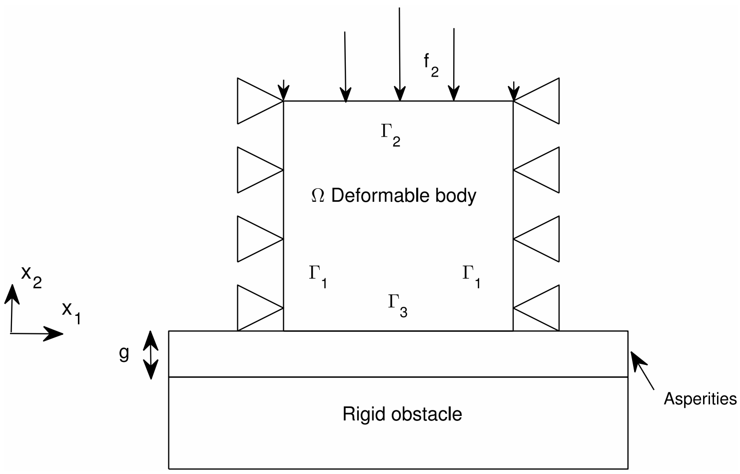

Fig. 9. Physical configuration for Example 6.3.

and $p(r)$ is the same function defined in Example 6.2. In Fig. 9, we see that the foundation is made of a rigid material covered by a layer composed of soft material, say asperities, with thickness g. From the contact boundary condition, we see that it follows a normal compliance condition as far as the penetration is less than the bound g, and it follows a unilateral constraint when the rigid obstacle is reached. For the numerical simulation, we choose $g = 0.02$ m, $\alpha = 40$ and $\beta = 0.5$, then we can observe the situation that the rigid obstacle is touched, i.e., $u_\nu > 0.02$.

To show the numerical convergence orders, we calculate the numerical solutions on a family of square meshes $\mathcal{T}^h$ with $h = 2^{-n}, 2, \ldots, 6$. The relative errors $\left\|\Pi_1(\boldsymbol{u}^h - \boldsymbol{u}_{ref})\right\|_{H^1} / \left\|\Pi_1 \boldsymbol{u}_{ref}\right\|_{H^1}$ and convergence orders are listed in Table 4. We clearly observe that the convergence order is nearly one, which again matches the theoretical prediction.

Table 4
Errors and numerical convergence orders of lowest-order VEM for Example 6.3.

h	2^{-2}	2^{-3}	2^{-4}	2^{-5}	2^{-6}
Errors	3.3572e−1	1.8988e−1	1.0312e−1	5.5324e−2	2.8768e−2
Convergence orders	–	0.82220	0.88070	0.89841	0.94343

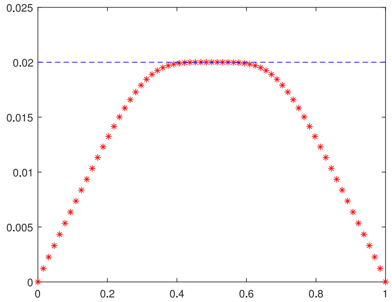

(a) normal displacement u_ν

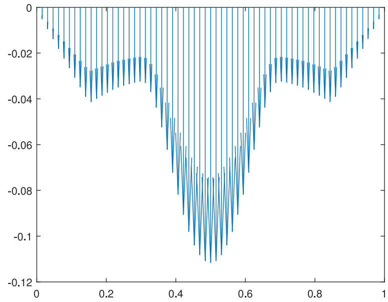

(b) normal stress σ_ν

Fig. 10. Numerical normal displacement and normal stress in Example 6.3.

In Fig. 10, we show the behaviors of the normal displacement u_ν and normal stress σ_ν on contact boundary Γ_3 of the numerical solution on the mesh with $h = 2^{-6}$. For $0 \le u_\nu < 0.01$ the normal stress increases with respect to the penetration, and for $0.01 \le u_\nu < 0.02$ it decreases. Furthermore, when the rigid obstacle is reached, i.e., $u_\nu = 0.02$, the normal stress is active.

Acknowledgments

We thank the two anonymous referees for their valuable comments and suggestions.

References

[1] G. Duvaut, J.-L. Lions, Inequalities in Mechanics and Physics, Springer-Verlag, Berlin, 1976.
[2] R. Glowinski, J.-L. Lions, R. Trémolières, Numerical Analysis of Variational Inequalities, North-Holland, Amsterdam, 1981.
[3] C. Baiocchi, A. Capelo, Variational and Quasivariational Inequalities: Applications to Free-Boundary Problems, John Wiley, Chichester, 1984.
[4] R. Glowinski, Numerical Methods for Nonlinear Variational Problems, Springer-Verlag, New York, 1984.
[5] N. Kikuchi, J.T. Oden, Contact Problems in Elasticity: A Study of Variational Inequalities and Finite Element Methods, SIAM, Philadelphia, 1988.
[6] I. Hlaváček, J. Haslinger, J. Necǎs, J. Lovíšek, Solution of Variational Inequalities in Mechanics, Springer-Verlag, New York, 1988.
[7] P.D. Panagiotopoulos, Nonconvex energy functions, hemivariational inequalities and substationary principles, Acta Mech. 42 (1983) 160–183.
[8] F.H. Clarke, Generalized gradients and applications, Trans. Amer. Math. Soc. 205 (1975) 247–262.
[9] F.H. Clarke, Optimization and Nonsmooth Analysis, Wiley, Interscience, New York, 1983.
[10] P.D. Panagiotopoulos, Hemivariational Inequalities, Applications in Mechanics and Engineering, Springer-Verlag, Berlin, 1993.
[11] Z. Naniewicz, P.D. Panagiotopoulos, Mathematical Theory of Hemivariational Inequalities and Applications, Marcel Dekker, Inc., New York, Basel, Hong Kong, 1995.
[12] S. Carl, V.K. Le, D. Motreanu, Nonsmooth Variational Problems and Their Inequalities: Comparison Principles and Applications, Springer, New York, 2007.
[13] S. Migórski, A. Ochal, M. Sofonea, Nonlinear inclusions and hemivariational inequalities, in: Models and Analysis of Contact Problems, in: Advances in Mechanics and Mathematics, vol. 26, Springer, New York, 2013.
[14] M. Sofonea, S. Migórski, Variational–Hemivariational Inequalities with Applications, Chapman & Hall/CRC Press, Boca Raton-London, 2018.
[15] J. Haslinger, M. Miettinen, P.D. Panagiotopoulos, Finite Element Method for Hemivariational Inequalities, in: Theory, Methods and Applications, Kluwer Academic Publishers, Boston, Dordrecht, London, 1999.
[16] W. Han, S. Migórski, M. Sofonea, A class of variational–hemivariational inequalities with applications to frictional contact problems, SIAM J. Math. Anal. 46 (2014) 3891–3912.
[17] W. Han, M. Sofonea, Numerical analysis of hemivariational inequalities in contact mechanics, Acta Numer. 28 (2019) 175–286.
[18] L. Beirão da Veiga, F. Brezzi, A. Cangiani, G. Manzini, L.D. Marini, A. Russo, Basic principles of virtual element methods, Math. Models Methods Appl. Sci. 23 (2013) 119–214.
[19] L. Beirão da Veiga, F. Brezzi, L.D. Marini, Virtual elements for linear elasticity problems, SIAM J. Numer. Anal. 51 (2013) 794–812.
[20] A.L. Gain, C. Talischi, G.H. Paulino, On the virtual element method for three-dimensional elasticity problems on arbitrary polyhedral meshes, Comput. Methods Appl. Mech. Engrg. 282 (2014) 132–160.
[21] E. Artioli, L. Beirão da Veiga, C. Lovadina, E. Sacco, Arbitrary order 2d virtual elements for polygonal meshes: part I. elastic problem, Comput. Mech. 60 (2017) 355–377.
[22] B. Zhang, J. Zhao, Y. Yang, S. Chen, The nonconforming virtual element method for elasticity problems, J. Comput. Phys. 378 (2019) 394–410.
[23] P. Wriggers, W.T. Rust, B.D. Reddy, A virtual element method for contact, Comput. Mech. 58 (2016) 1039–1050.
[24] F. Wang, H. Wei, Virtual element method for simplified friction problem, Appl. Math. Lett. 85 (2018) 125–131.
[25] F. Wang, H. Wei, Virtual element methods for obstacle problem, IMA J. Numer. Anal. 40 (2020) 708–728.

[26] F. Feng, W. Han, J. Huang, Virtual element methods for elliptic variational inequalities of the second kind, J. Sci. Comput. 80 (2019) 60–80.
[27] F. Wang, J. Zhao, Conforming and nonconforming virtual element methods for a kirchhoff plate contact problem, IMA J. Numer. Anal. (2020) http://dx.doi.org/10.1093/imanum/draa005.
[28] F. Feng, W. Han, J. Huang, Virtual element method for an elliptic hemivariational inequality with applications to contact mechanics, J. Sci. Comput. 81 (2019) 2388–2412.
[29] Z. Denkowski, S. Migórski, N.S. Papageorgiou, An Introduction to Nonlinear Analysis: Theory, Kluwer Academic/Plenum Publishers, Boston, Dordrecht, London, New York, 2003.
[30] W. Han, M. Sofonea, M. Barboteu, Numerical analysis of elliptic hemivariational inequalities, SIAM J. Numer. Anal. 55 (2017) 640–663.
[31] L. Beirão da Veiga, C. Lovadina, A. Russo, Stability analysis for the virtual element method, Math. Models Methods Appl. Sci. 27 (2017) 2557–2594.
[32] S.C. Brenner, L.R. Scott, The Mathematical Theory of Finite Element Methods, third ed., Springer-Verlag, New York, 2008.
[33] W. Han, M. Sofonea, Quasistatic Contact Problems in Viscoelasticity and Viscoplasticity, in: Studies in Advanced Mathematics, vol. 30, Americal Mathematical Society, RI–International Press, Providence, Somerville, MA, 2002.
[34] L. Beirão da Veiga, C. Lovadina, D. Mora, A virtual element method for elastic and inelastic problems on polytope meshes, Comput. Methods Appl. Mech. Engrg. 295 (2015) 327–346.
[35] H. Chi, L. Beirão da Veiga, G.H. Paulino, Some basic formulations of the virtual element method (vem) for finite deformations, Comput. Methods Appl. Mech. Engrg. 318 (2017) 148–192.
[36] M. Ling, F. Wang, W. Han, The nonconforming virtual element method for a stationary stokes hemivariational inequality with slip boundary condition, J. Sci. Comput. 85 (2020) 56.
[37] K. Atkinson, W. Han, Theoretical Numerical Analysis: A Functional Analysis Framework, third ed., Springer-Verlag, New York, 2009.
[38] M. Barboteu, K. Bartosz, W. Han, T. Janiczko, Numerical analysis of a hyperbolic hemivariational inequality arising in dynamic contact, SIAM J. Numer. Anal. 53 (2015) 527–550.
[39] M. Barboteu, K. Bartosz, P. Kalita, An analytical and numerical approach to a bilateral contact problem with nonmonotone friction, Int. J. Appl. Math. Comput. Sci. 23 (2013) 263–276.
[40] M. Barboteu, K. Bartosz, P. Kalita, A. Ramadan, Analysis of a contact problem with normal compliance, finite penetration and nonmonotone slip dependent friction, Commun. Contemp. Math. 16 (2014) 1350016.
[41] W. Han, M. Sofonea, D. Danan, Numerical analysis of stationary variational–hemivariational inequalities, Numer. Math. 139 (2018) 563–592.